Turkish Journal of Engineering

Turkish Journal of Engineering (TUJE)
Vol. 1, Issue 2, pp. 1-8, September 2017
ISSN 2587-1366, Turkey
DOI

MINERALOGICAL, GEOCHEMICAL AND MICROMORPHOLOGICAL CHARACTERISTICS OF CALCITE PRECIPITATED FROM A THIN COVER OF RECENT WATER TAKEN FROM THE STALAGMITES IN KÜPELI CAVE, ESENPINAR (ERDEMLI, MERSIN), SOUTHERN TURKEY

Muhsin Eren *[1], Selahattin Kadir [2] and Murat Akgöz [3]

[1] Mersin University, Engineering Faculty, Department of Geological Engineering, Mersin, Turkey (m_eren@yahoo.com)

[2] Eskisehir Osmangazi University, Faculty of Engineering and Architecture, Department of Geological Engineering, Eskişehir, Turkey (skadir.esogu@gmail.com)

[3] General Directorate of Mineral Research and Exploration (MTA), Ankara, Turkey (murat_akgoz@yahoo.com)

* Corresponding Author
Received: 13/04/2017 Accepted: 16/05/2017

ABSTRACT
Küpeli cave in southern Turkey (UTM: 36.606085 ºN, 34.114917 ºE, 742 m asl) shows recent stalagmite development at several points beneath dripping water on a stack of blocks due to collapse of the cave ceiling. Calcite precipitated from water supersaturated with respect to $CaCO_3$ under the surface conditions taken from a thin cover of water on the upper surface of stalagmites was analysed using the several analytical techniques, including XRD, DTA-TG, IR, ICP-OES and MS and stable isotope analyses. The results revealed that the precipitated material consists almost entirely of calcite. In the SEM images, the precipitate is composed mainly of euhedral to subhedral equant calcite crystals with size of 5-10 µm and an interwoven mass of calcite filaments. Stable isotope values of the calcite ($\delta^{18}O$ = –3.81 ‰ V-PDB and $\delta^{13}C$ = –6.92 ‰ V-PDB) indicate precipitation from meteoric soil water. The crystalline fabric of the precipitate points out inorganic precipitation whereas filamentous forms suggest calcified green algae at advance stage of evaporation.

Keywords: *Newly Forming Calcite, Mineralogy, Micromorphology, Geochemistry, Küpeli Cave, Southern Turkey*

1. INTRODUCTION

Stalagmite is a type of speleothem that grows upward on the floor of a cave beneath dripping water. Cave deposits have received a great interest of researchers working on karst formation. Most studies mainly focus on stable isotope composition ($\delta^{18}O$ and $\delta^{13}C$) of cave calcite used for paleoclimatic reconstructions (e.g., Lauritzen and Lundberg, 1999; Vaks et al., 2003, 2010; McDermott, 2004; Johnson et al., 2006; Verheyden et al., 2008; Dominguez-Villar et al., 2008; Tremaine et al., 2011). Speleothems also provide information on soil/vegetation dynamics, hydrological conditions, annual lamination, growth rate and dating, organic acid contents and atmospheric changes (McDermott, 2004; Fairchild and Treble, 2009 and for other references). There is little information available considering recent cave deposits. Previous studies on recent speleothems focus on dating (Gascoyne and Nelson, 1983; Baskaran and Iliffe, 1993), growth rates (Baker and Smart, 1995; Baker et al., 1998; Genty et al., 2001; Sherwin and Baldini, 2011), factors affecting calcite growth and fabric (Turrero et al., 2009) and stable isotope composition (Riechelmann et al., 2013). In addition, Day and Henderson (2011) investigate oxygen isotope in calcite grown under cave-analogue conditions. Therefore, this study investigates mineralogy, geochemistry, stable isotope chemistry and micromorphology of newly forming calcite precipiated from a thin cover of water taken from the stalagmites, and provides some new data for recent cave deposits.

2. STUDY SETTING

2.1. Location and climate

Küpeli Cave is located at latitude 599726 E and longitude 4051941 N (UTM: 36.606085 ^{o}N, 34.114917 ^{o}E) and an elevation of 742 m in southern Turkey, about 1.7 km northeast of Esenpınar (Erdemli/Mersin; Figures 1, 2). This location takes a place within the Tauride orogenic belt where platform carbonates are common. Küpeli Cave was developed within the reefal limestone of the Mut Formation (Langian-Serravalian) in which red algae and corals are common (Figure 3; Gedik et al., 1979; Eren, 2008). Mediterranean-type semi-arid climate prevails at outside of the cave, characterized by the mean annual values of precipitation (634 mm), evaporation (1321 mm) and temperature (18.7 °C) obtained from the meteorological measurements of 70-years (Eren et al., 2008).

2.2. Geology

In the region, karstification is very common, and has been developed in carbonates at skirts of the Tauride Mountains where hundreds of caves including Küpeli Cave can be found with different features and processes (Akgöz and Eren, 2015). Karstification in the region probably started after emergence of the Central Taurides due to epeirogenetic raise at the end of Miocene. Following the raise, karstification was deepened due to dry and hot climate. In the region, extension of karstic surface features and distribution of caves show

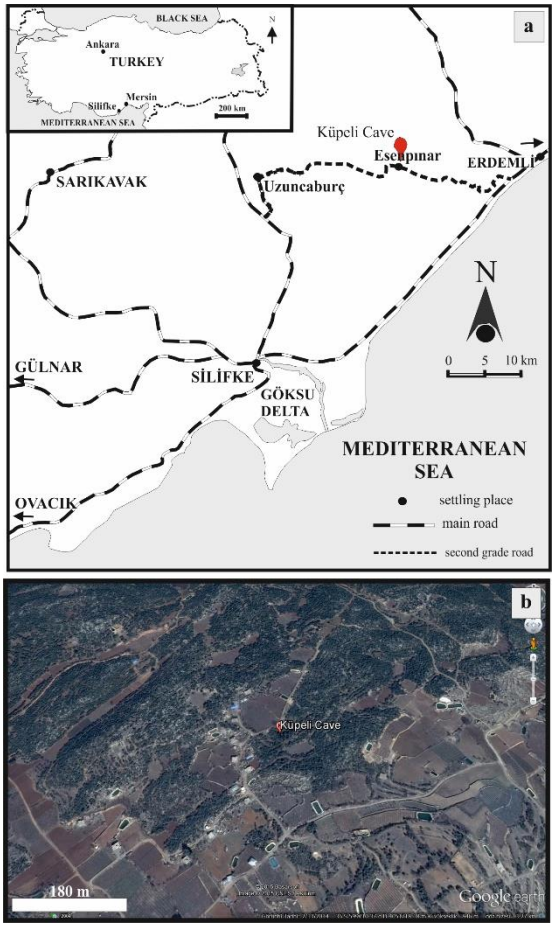

Figure 1. Location map (a) and satellite image (b) showing location of Küpeli Cave marked in red.

consistency with the distinctive tectonic lines which indicates the effect of tectonics on karstification. Karstification in the area, especially caves largely developed and shaped along NW-SE direction due to effects of discontinuities. The majority of the caves were developed at NW-SE direction (Akgöz, 2012; Akgöz and Eren, 2015).

2.3. Cave description

Küpeli Cave consists of two chambers which are connected with each other with a narrow passage (Figure 4). The first chamber is 30 m long, 20 m wide and 0.4 to 42 m in height. Entrance to the first chamber is provided by stairs from the collapsed portion of the roof (Figure 5 a). Whereas, the second chamber is of a smaller size being 17 m long, 9 m wide and 38 m in height. In the second room, speleothems are common. The first chamber is very poor in terms of cave deposits, however, several stalagmite development beneath dripping water was observed on the pile of broken parts below the collapsed portion of the cave cealing (Figure 5 b-e).

3. MATERIALS AND METHODS

Only one calcium-rich water sample was taken by careful scraping with a sharp knife from upper surface of

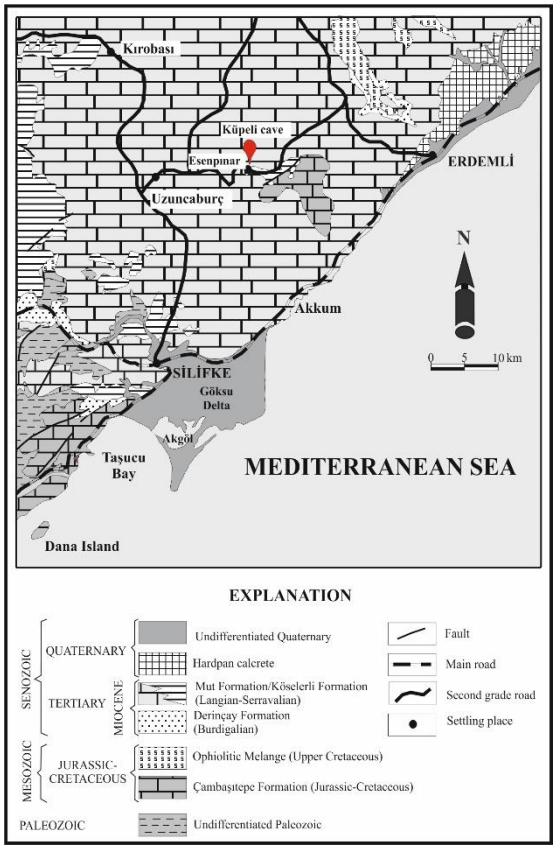

Figure 2. Geological map of the study area where Küpeli Cave is marked in red (Eren, 2008).

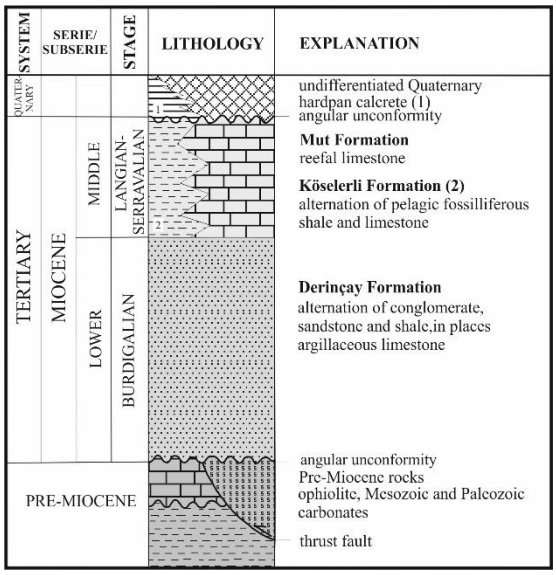

Figure 3. Generalized stratigraphical column of the study area.

the stalagmites, and the water sample was kept in a glass sample holder. The water sample was then left for precipitation of calcite under the surface conditions including a surface temperature of 36 ^{o}C during the summer time. We were not able to take dripping water sample because of its very low dripping rate. The precipitated material with a weight of 270 mg was

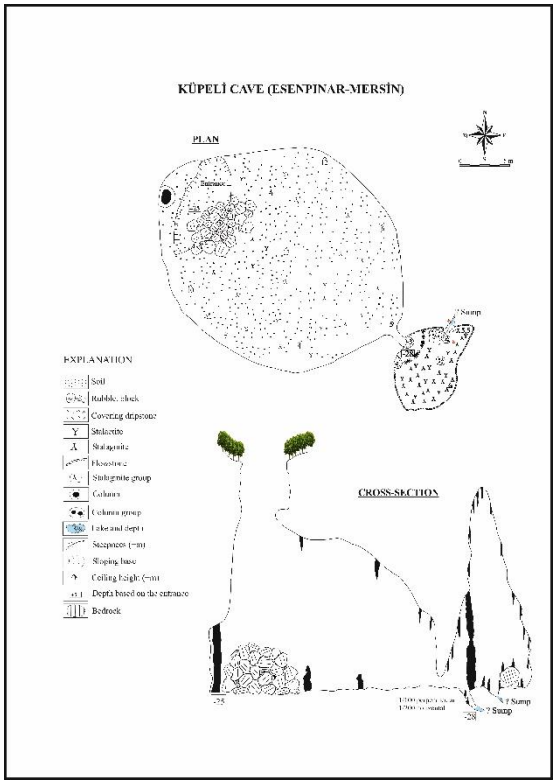

Figure 4. Plan view and vertical section of Küpeli Cave.

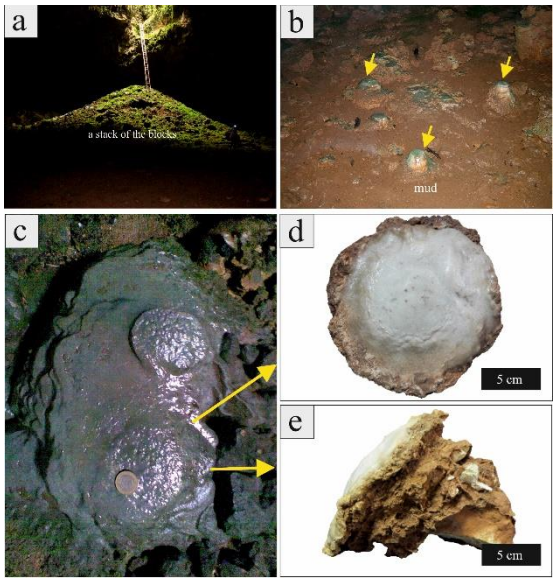

Figure 5. (a) Küpeli Cave entrance and a stack of blocks on the floor covered by green alga beneath the collapse of the cave ceiling; (b) recent stalagmites (arrow) developing on the skirt of the stack (a); (c) close view of the two recent stalagmites on the stack covered by a thin film of water and also by green algae (green colour); (d) and (e) are top and longitudinal views of the recent stalagmite, respectively. The stalagmite is covered by newly formed calcite in white colour (d).

characterized using a range of analytical techniques. Mineralogical characteristics of the precipitated material were determined by XRD analysis using a Rigaku D /

Max – 2200 Ultia PC instrument with CuKα radiation and a scanning speed of 1º2θ min^{-1}. SEM-EDX analysis was performed using a JEOL JSM 5600LV instrument with an EDX detector. For SEM-EDX analysis, a piece of the precipitate was placed by adhering onto an aluminum sample holder with double-sides and coated with a film (~350 Å) of gold using a Giko ion coater. Differential thermal and thermogravimetry analyses (DTA-TG) (PerkinElmer – Pyris 1, USA) were obtained from the 10 mg of the powdered precipitated material in a Pt sample holder, heated at an average rate of 10°C/min with an alumina reference. IR spectroscopic analysis was carried out on the pressed powder sample with a size of less than 2 μm mixed with KBr using a PerkinElmer 100 FT-IR spectrometer, and scan was run at 4 cm^{-1} resolution.

The calcite precipitate was analysed for selected major and trace elements using both inductively coupled plasma-optical emmission spectroscopy (ICP-OES) and inductively coupled plasma-mass spectroscopy (ICP-MS) methods in the Analytical Services Laboratory of the University of Greenwich (London, United Kingdom). This method was conducted after dissolution using a lithium metaborate fusion (Jarvis and Jarvis, 1992). In essence, 0.25 g of the sample was mixed with 1.25 g of lithium metaborate flux and fused at 900 °C. The molten bead was poured into weak nitric acid and stirred until dissolved. The resultant solution was made to volume. The analysis of major elements and some trace elements was undertaken using a Thermo ICAP 6500 ICP-OES with calibration via matrix-matched synthetic standards. Analysis of the remaining trace elements was completed using a Thermo X series 2 ICP-MS, again with calibration via matrix-matched synthetic standards and the use of CRMs and internal QC powders.

4. RESULTS

4.1. XRD determinations

The mineralogical composition of the precipitated material was determined by X-ray diffractometry. The results show that the precipitated material consists entirely of calcite identified by peaks at 3.87, 3.04, 2.85, 2.50, 2.29, 2.10, 2.92, and 2.88 Å (Figure 6).

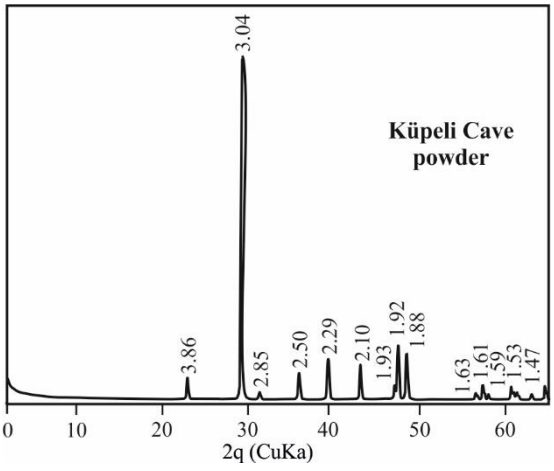

Figure 6. XRD patterns of newly formed calcite crystal from Küpeli cave.

4.2. SEM-EDX analysis

SEM analyses were carried out on the precipitate that typically occurs as euhedral to subhedral equant calcite crystals with size of 5-10 μm and filaments (Figure 7a-e). The filaments of the interwoven network have a length of approximately 10–20 μm and a width up to 1 μm, extending between the calcite crystals (Figure 7d-e). The EDX spectra of the crystals and filaments show strong peaks of Ca confirming the calcite composition (Figure 7f).

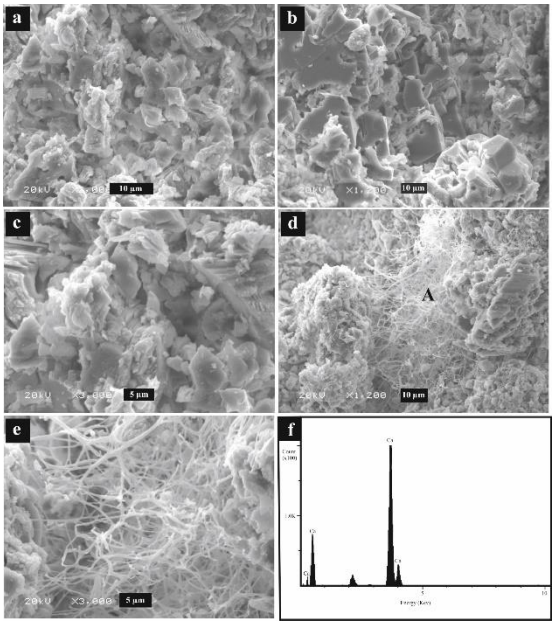

Figure 7. SEM images showing (a-c) newly formed calcite composed of euhedral and subhedral crystals; (d) filamentous green algae associated calcite crystals; (e) close view of (d); (f) EDX spectrum of newly formed calcite showing Ca peaks.

4.3. DTA-TG determinations

The DTA-TG curves of the calcite precipitate have a large endothermic peak at about 874°C (weight loss 46%) due to the decomposition of the calcite crystal structure (Figure 8). The result is consistent with those of stated by MacKenzie (1957), Webb and Krüger (1970) and Smykatz-Kloss (1974).

4.4. IR spectra

The IR spectra of the calcite sample is recognized by a diagnostic broad, intense band at 1417 cm^{-1} and sharp bands at 874 and 712 cm^{-1} corresponding to stretching vibration of the CO_3^{-2} anions, out-of-plane bending mode, and in-plane bending vibrations, respectively (Figure 9; Van der Marel and Beutelspacher, 1976; Madejová et al., 2011).

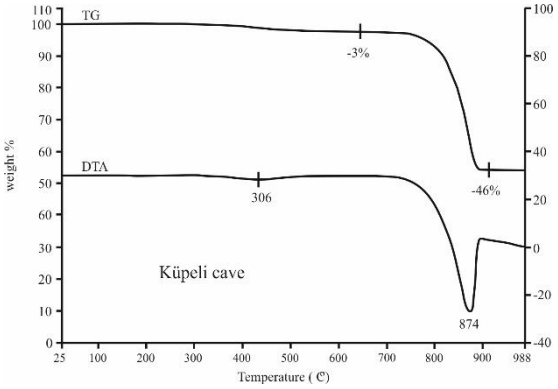

Figure 8. DTA-TG curves for newly formed calcite crystal from Küpeli cave.

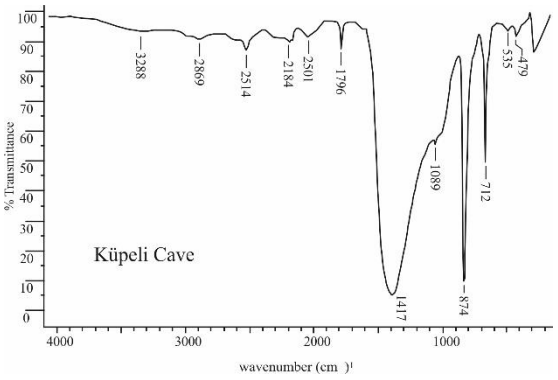

Figure 9. IR spectrum of newly formed calcite crystal from Küpeli cave.

4.5. Chemical Analysis

Chemical analysis of the precipitated material revealed that the precipitate is composed mainly of CaO (54.39 wt.%) and LOI (44.32 wt.%), and includes trace amount of SiO_2, Al_2O_3, Fe_2O_3, TiO_2, K_2O, MgO, Na_2O, P_2O_5, Mn, Ba, and Sr (Table 1). The chemical analysis are consistent with the results of XRD, SEM-EDX, DTA-TG and IR.

Table 1 Chemical composition of the precipitated calcite.

CaO wt.%	SiO_2 wt.%	Al_2O_3 wt.%	Fe_2O_3 wt.%	TiO_2 wt.%	K_2O wt.%	MgO wt.%
54.39	0.69	0.28	0.18	0.02	0.03	0.05

Na_2O wt.%	P_2O_5 wt.%	LOI wt.%	Total wt.%	Mn mg/kg	Sr mg/kg	Ba mg/kg
0.01	0.07	44.32	100.04	16	70	7.4

4.6 Stable isotope analysis

Stable isotope analysis was performed on the calcite precipitate. The results given in Table 2 indicate that $\delta^{18}O$ and $\delta^{13}C$ values of the calcite are –3.81 and –6.92 ‰ V-PDB, respectively.

Table 2. Stable isotope composition of the newly formed calcite.

$\delta^{18}O_{V\text{-}PDB}$ (‰)	$\delta^{13}C_{V\text{-}PDB}$ (‰)
–3.81	–6.92

5. DISCUSSION

Calcium carbonate is generally precipitated as calcite crystals in water supersaturated with respect to $CaCO_3$. In this study, supersaturated water covering the upper surface of the stalagmites was scraped, then left to precipitate in a glass sample holder under the surface conditions including a surface temperature of 36 ºC where evaporation increased concentration (activity) of Ca ions, and then caused precipitation of $CaCO_3$. In the cave environment, precipitation conditions are probably provided during the dry seasons, and controlled by many factors such as temperature, water supply, humidity, and pCO_2 level (Day and Henderson, 2011). Calcium carbonate precipitation occurs by the reaction:

$$Ca^{2+} + 2HCO_3^- \rightarrow CaCO_3 + H_2O + CO_2$$

XRD and DTA-TG analyses revealed that the precipitated material is pure calcite showing all characteristic peaks. However, very low values of SiO_2, Al_2O_3, K_2O, MgO indicates presence of trace amount of impurities such as clay in the sample derived either from wind-blown dust or surface. Low Sr and Ba values are consistent with those of cave calcite (Sr 34–256 ppm and Ba < 40 ppm) (ongoing study in the same area; Verheyden et al., 2000; Fairchild et al., 2010; Wassenburg et al., 2012) and terrestrial (freshwater) sediments (Chen et al., 1997; Eren et al., 2008 for calcretes). Trace element contents in speleothems reflect water-rock and soil interaction time which is controlled by hydrological conditions and partitioning of the element from the water during calcite precipitation (Verheyden, 2004; Wassenburg et al., 2012; Vuai, 2012; Huang and Fairchild, 2001).

The $\delta^{18}O$ and $\delta^{13}C$ values of the precipitated calcite are –3.81 ‰ V-PDB and –6.92 ‰ V-PDB, respectively. The $\delta^{18}O$ value indicates precipitation from meteoric water, and is higher than those (mean –5.38 ‰ V-PDB) measured in speleothems (ongoing study in the Mersin area). Dominguez-Villar et al. (2008) and Day and Henderson (2011) reported mean $\delta^{18}O$ values of –6.25 and –6.82 ‰ V-PDB for speleothems from Kaite Cave, northern Spain and for calcite grown under the cave-analogue conditions with drip rate of 1.6 drips/min, respectively. Similar $\delta^{18}O$ values are reported by Riechelmann et al. (2013) as –5.6 to –6.3 ‰ V-PDB for watch glass calcite samples with different drip rate in the cave environment. The oxygen isotopic fractionation between water and carbonates is mainly temperature dependent (Poulson and White, 1969; Friedman and O'Neil, 1977; Talbot and Kelts, 1990; Lachniet, 2009; Deocampo, 2010). Since enrichment in the $\delta^{18}O$ value of the precipitated calcite relative to those of the speleothem in the Mersin area and its counterparts in the literature is due to evaporation.

The $\delta^{13}C$ value of the precipitated calcite is within the range of those of speleothems (ongoing study in the Mersin area; Bar-Matthews et al., 1997; McDermott, 2004) and also calcretes (Eren et al., 2008; Eren, 2011; Kaplan et al., 2013) indicating a contribution of light CO_2 from the soil into percolating water due to reactions such as the root respiration and organic matter decomposition (Sherwin and Baldini, 2011).

Euhedral and subhedral calcite crystals in the SEM images with the $\delta^{18}O$ and $\delta^{13}C$ values indicate slow inorganic precipitation process from soil water by evaporation. However, presence of algal filaments in the SEM views may suggests another mechanism which is photosynthetic removal of CO_2 (Cox et al., 1989). However, a network of algal filaments on the calcite crystals in local areas suggest that main mechanism is inorganic precipitation by which algal filaments were rapidly calcified at intense evaporation stage as final product of deposition (Jones and Kahle, 1993; Northup and Lavoie, 2001). In caves, loss of CO_2 by diffusion from supersaturated solutions is the major cause of calcium carbonate precipitation (Cox et al., 1989). Under conditions where cave-air PCO_2 is set at atmospheric levels, the supersaturation of fluid, and hence the growth depends mainly on the Ca content of water (Fairchild and McMillan, 2007) mainly controlled by evaporation rate. In the cave environment, evaporation is very slow compared to outside because of high moisture that causes massive macro-crystalline calcite in speleothem such as stalamigtites (ongoing study; Bar-Matthews et al., 1997) that differs from crystal morphologies of the calcite precipitated from a thin cover of water under surface conditions.

6. CONCLUSION

Newly forming calcite precipitated from water supersaturated with respect to $CaCO_3$ taken from a thin cover of water on the upper surface of stalagmites was analysed using a range of analytical techniques. XRD, IR, DTA-TG, and ICP-OES and ICP-MS analyses show that the precipitate consists almost entirely of calcite. SEM images revealed that the calcite precipitate mainly occurs as euhedral to subhedral equant crystals, and also includes green algal filaments extending between calcite crystals. The crystalline fabric and stable isotope values ($\delta^{18}O$ and $\delta^{13}C$) suggest slow inorganic precipitation from meteoric soil water. The algal filaments reflect rapid calcification at intense period of evaporation. Fabric difference between newly forming calcite and speleothems can be explained by environmental differences. In caves, calcite precipitation takes place under the high humidity and feedback or drip water mechanism whereas our sample characterizes precipitation under surface conditions where evaporation was dominant.

REFERENCES

Akgöz, M. (2012). Göksu nehri ve Lamas kanyonu (Mersin) arasında kalan bölgenin karst evrimi, PhD Thesis, Mersin University, Mersin, Turkey.

Akgöz, M. and Eren, M. (2015). Traces of earthquakes in the caves: Sakarlak Ponor and Kepez Cave, Mersin (S Turkey). Journal of Cave and Karst Studies, Vol. 77, No. 1, 63–74.

Baker, A. and Smart, P. L. (1995). Recent flowstone growth rates: Field measurements in comparison to theoretical predictions. Chemical Geology, Vol. 122, 121–128.

Baker, A., Genty, D., Dreybrodt, W., Barnes, W. L., Mockler, N. J. and Grapes, J. (1998). Testing theoretically predicted stalagmite growth rate with Recent annually laminated samples: Implications for past stalagmite deposition. Geochimica et Cosmochimica Acta, Vo. 62, No. 3, 393–404.

Bar-Matthews, M., Ayalon, A. and Kaufman, A. (1997). Late Quaternary Paleoclimate in the Eastern Mediterranean Region from Stable Isotope Analysis of Speleothems at Soreq Cave, Israel. Quaternary Research, Vol. 47, No. 2, 155–168.

Baskaran, M. and Iliffe, T. M. (1993). Age determination of recent cave deposits using excess 210Pb- a new technique. Geophysical Research Letter, Vol. 20, No. 7, 603–606.

Chen, Z., Chen, Z. and Zhang, W. (1997). Quaternary stratigraphy and trace-element indices of the Yangtze Delta, Eastern China, with special reference to marine transgressions. Quaternary Research, Vol. 47, No. 2, 181–191.

Cox, G., James, J. M., Armstrong, R. A. L. and Leggett, K. E. A. (1989). Stromatolotic crayfish-like stalagmites. Proceedings of the University of Bristol Spelaeological Society 18, pp. 339–358.

Day, C. C. and Henderson, G. M. (2011). Oxygen isotopes in calcite grown under cave-analogue conditions. Geochimica et Cosmochimica Acta, Vol. 75, No. 14, 3956–3972.

Deocampo, D. M. (2010). Geochemistry of continental carbonates. In: Alonso-Zarza, A.M. and Tanner, L.H., Eds., Carbonates in continental settings: geochemistry, diagenesis, and applications. Amsterdam, Netherland, Elsevier, Developments in Sedimentology 62, pp. 1–59.

Domínguez-Villar, D., Wang, X., Cheng, H., Martín-Chivelet, J. and Edwards, R. L. (2008). A high-resolution late Holocene speleothem record from Kaite Cave, northern Spain: $\delta^{18}O$ variability and possible causes. Quaternary International, Vol. 187, No. 1, 40–51.

Eren, M., 2008. Olba (Ura-Uğuralanı) jeoarkeolojisi (Silifke, Mersin). Ankara, Kültür ve Turizm Bakanlığı 24. Arkeometri Sonuçları Toplantısı, 181–192.

Eren, M. (2011). Stable isotope geochemistry of Quaternary calcretes in the Mersin area, southern Turkey - A comporasion and implications for their origin. Chemie der Erde, Vol. 71, No. 1, 31–37.

Eren, M., Kadir, S., Hatipoğlu, Z. and Gül, M. (2008). Quaternary calcrete development in the Mersin area, southern Turkey. Turkish Journal of Earth Sciences, Vol. 17, No. 4, 763–784.

Fairchild, I. J. and McMillan, E.A. (2007). Speleothems as indicators of wet and dry periods. International Journal of Speleology, Vol. 36, No. 2, 69-74.

Fairchild, I. J. and Treble, P. C. (2009). Trace elements in speleothems as recorders of environmental change. Quaternary Science Reviews, Vol. 28, No. 5-6, 449–468.

Fairchild, I. J., Spötl, C., Frisia, S., Borsato, A., Susini, J., Wynn, P. M., Cauzid, J. and EIMF (2010). Petrology and geochemistry of annually laminated stalagmites from an Alpin Cave (Obir, Austria): Seasonal cave physiology. Geological Society, London, Special Publications 336, 295–321.

Friedman, I. and O'Neil, J. R. (1977). Compilation of stable isotope factors of geochemical interest. In: Fleischer, M., Ed., Data of Geochemistry. United States Geological Survey Professional Paper 440-KK, pp. 1–12.

Gascoyne, M. and Nelson, D. E. (1983). Growth mechanisms of recent speleothems from Castleguard Cave, Columbia Icefields, Alberta, Canada, inferred from a comparison of uranium-series and carbon-14 age data. Arctic and Alpine Research, Vol. 15, No. 4, 537–542.

Gedik, A., Birgili, Ş., Yılmaz, H. and Yoldaş, R. (1979). Mut-Ermenek-Silifke yöresinin jeolojisi ve petrol olanakları. Türkiye Jeoloji Kurumu Bülteni, Vol. 22, No.1, 7–26.

Genty, D., Baker, A. and Vokal, B. (2001). Intra- and inter-annual growth rate of modern stalagmites. Chemical Geology, Vol. 176, No. 1-4, 191–212.

Huang, Y. and Fairchild, I. J. (2001). Partitioning of Sr^{2+} and Mg^{2+} into calcite under karst-analogue experimental conditions. Geochimica et Cosmochimica Acta, Vol. 65, No. 1, 47–62.

Jarvis, I. and Jarvis, K. E. (1992). Plasma spectrometry in earth sciences: techniques, applications and future trends. In: Jarvis, I. and Jarvis, K.E., Eds., Plasma spectrometry in Earth Sciences. Chemical Geology 95, pp. 1–33.

Johnson, K. R., Hu, C., Belshaw, N. S. and Henderson, G. M. (2006). Seasonal trace-element and stable-isotope variations in a Chinese speleothem: The potential for high-resolution paleomonsoon reconstruction. Earth and Planetary Science Letters, Vol. 244, No. 1-2, 394–407.

Jones, B. and Kahle, C. F. (1993). Morphology, relationship, and origin of fiber and dendritic calcite crystals. Journal of Sedimentary Petrology, Vol. 63, No. 6, 1018–1031.

Kaplan, M. Y., Eren, M., Kadir, S. and Kapur, S. (2013). Mineralogical, geochemical and isotopic characteristics of Quaternary calcretes in the Adana region, southern Turkey: Implications on their origin. Catena, Vol.101, 164–177.

Lachniet, M. S. (2009). Climatic and environmental controls on speleothem oxygen-isotope values. Quaternary Science Reviews, Vol. 28, No. 5-6, 412–432.

Lauritzen, S. T. and Lundberg, J. (1999). Speleothems and climate: a special issue of The Holocene. Holocene Vol. 9, No. 6, 643–647.

MacKenzie, R. C. (1957). The Differential Thermal Investigation of Clays. Mineralogical Society, London, UK.

Madejová, J., Balan, E. and Petit, S. (2011). Application of vibrational spectroscopy to the characterization of phyllosilicates and other industrial minerals. EMU Notes in Mineralogy, Vol. 9, pp 171–226.

McDermott, F. (2004). Palaeo-climate reconstruction from stable isotope variations in speleothems: a review. Quaternary Science Reviews, Vol. 23, No. 7-8, 901–918.

Northup, D.E. and Lavoie, K.H., 2001. Geomicrobiology of caves: a review. Geomicrobiology Journal, Vol. 18, No. 3, 199–222.

Poulson, T. L. and White, W. B. (1969). The cave environment. Science, Vol. 165, No. 3897, 971–981.

Riechelmann, D. F. C., Deininger, M., Scholz, D., Riechelmann, S., Schröder-Ritzrau, A., Spötl, C., Richter, D. K., Mangini, A. and Immenhauser, A. (2013). Disequilibrium carbon and oxygen isotope fractionation in recentcave calcite: Comparison of cave precipitates and model data. Geochimica et Cosmochimica Acta, Vol. 103, 232–244.

Sherwin, C. M. and Baldini, J. U. L. (2011). Cave air and hydrological controls on prior calcite precipitation and stalagmite growth rates: Implications for palaeoclimate reconstructions using speleothems. Geochimica et Cosmochimica Acta, Vol.75, No. 14, 3915–3929.

Smykatz-Kloss, W., 1974. Differential Thermal Analysis: Application and Results in Mineralogy. Springer, Berlin.

Talbot, M.R. and Kelts, K., 1990. Paleolimnological signatures from carbon and oxygen isotopic ratios in carbonates from organic carbonrich lacustrine sediments. In: Katz, B.J., Ed., Lacustrine Basin Exploration: Case Studies and Modern Analogs. Tulsa, Oklohama, USA: American Association Petroleum Geologist Memoir 50, pp. 88–112.

Tremaine, D.M., Froelich, P.N. and Wang, Y., 2011. Speleothem calcite farmed in situ: Modern calibration of $\delta^{18}O$ and $\delta^{13}C$ paleoclimate proxies in a continuously-

monitored natural cave system. Geochimica et Cosmochimica Acta, Vol. 75, No. 17, 4929–4950.

Turrero, M.J., Garrolon, A., Gomez, P., Martin-Chivelet, J., Sanchez, L. and Ortega, A.I., 2009. Present-day calcite deposition in two caves of N Spain (Kaite and Cueva Mayor): Factors affecting calcitegrowth and fabric. Geochimica et Cosmochimica Acta, Vol. 73, Supplement A1356.

Vaks, A., Bar-Matthews, M., Ayalon, A., Schilman, B., Gilmour, M., Hawkesworth, C.J., Frumkin, A., Kaufman, A. snd Matthews, A., 2003. Paleoclimate reconstruction based on the timing of speleothem growth and oxygen and carbon isotope composition in a cave located in the rain shadow in Israel. Quaternary Research, Vol. 59, No. 2, 182–193.

Vaks, A., Bar-Matthews, M., Matthews, A., Ayalon, A. and Frumkin, A., 2010. Middle-Late Quaternary paleoclimate of northern margins of the Saharan-Arabian Desert: reconstruction from speleothems of Negev Desert, Israel. Quaternary Science Reviews, Vol. 29, No. 19-20, 2647–2662.

Van der Marel, H.W. and Beutelspacher, H., 1976. Atlas of Infrared Spectroscopy of Clay Minerals and Their Admixtures. Amsterdam, Netherland:Elsevier.

Verheyden, S., 2004. Trace elements in speleothems- A short review of the state of art. International Journal of Speleology, Vol. 33, No 1/4, 95–101.

Verheyden, S., Keppens, E., Fairchild, I.J., McDermott, F. and Weis, D., 2000. Mg, Sr and Sr isotope geochemistry of a Belgian Holocene speleothem: implications for paleoclimate reconstructions. Chemical Geology, Vol. 169, No. 1-2, 131–144.

Verheyden, S., Nader, F.H., Cheng, H.J., Edwards, L.A. and Swennen, R., 2008. Paleoclimate reconstruction in the Levant region from the geochemistry of a Holocene stalagmite from the Jeita cave, Lebanon. Quaternary Research, vol. 70, No. 3, 368-381.

Vuai, S.A.H., 2012. Geochemical Characteristics of Spaleotherm Formation in Caves from Zanzibar Island, Tanzania. 1:505. doi:10.4172/scientificreports.505.

Wassenburg, J.A., Immenhauser, A., Richter, D.K., Jochum, K.P., Fietzke, J., Deininger, M., Goos, M., Scholz, D. and Sabaoui, A., 2012. Climate and cave control on Pleistocene/Holocene calcite-to-aragonite transitions in speleothems from Morocco: Elemental and isotopic evidence. Geochimica et Cosmochimica Acta, Vol. 92, 23–47.

Webb, T.L. and Krüger, J.E., 1970. Carbonates. In: MacKenzie, R.C., Ed., Differential Thermal Analysis Vol. 1 - Fundamental Aspects. Academic Press, London.